Inorganic Chemistry

Article

pubs.acs.org/IC

Infrared Spectroscopic and Theoretical Investigations of the OUF_2 and $OThF_2$ Molecules with Triple Oxo Bond Character

Yu Gong,[†] Xuefeng Wang,[†,‡] Lester Andrews,*[,†] Tobias Schlöder,[§] and Sebastian Riedel[§]

[†]Department of Chemistry, University of Virginia, Charlottesville, Virginia 22904-4319, United States

[‡]Department of Chemistry, Tongji University, Shanghai, P.R. China 200092

[§]Institut für Anorganische und Analytische Chemie, Albert-Ludwigs Universität Freiburg, Albertstrasse 21, D-79104 Freiburg i. Br., Germany

Supporting Information

ABSTRACT: The terminal oxo species OUF_2 and $OThF_2$ have been prepared via the spontaneous and specific OF_2 molecule reactions with laser ablated uranium and thorium atoms in solid argon and neon. These isolated molecules are characterized by one terminal M-O and two F−M−F (M = U or Th) stretching vibrational modes observed in matrix isolation infrared spectra, which are further supported by density functional frequency calculations and CASPT2 energy and structure calculations. Both molecules have pyramidal structures with singlet (Th) and triplet (U) ground states. The molecular orbitals and metal−oxygen bond lengths for the OUF_2 and $OThF_2$ molecules indicate triple bond character for the terminal oxo groups, which are also substantiated by NBO analysis at the B3LYP level and by CASPT2 molecular orbital calculations. Dative bonding involving $O_{2p} \rightarrow Th_{6d}$ and U_{df} interactions is clearly involved in these oxoactinide difluoride molecules. Finally, the weak O−F bond in OF_2 as well as the strong U−O, U−F and Th−O, Th−F bonds make reaction to form the OUF_2 and $OThF_2$ molecules highly exothermic.

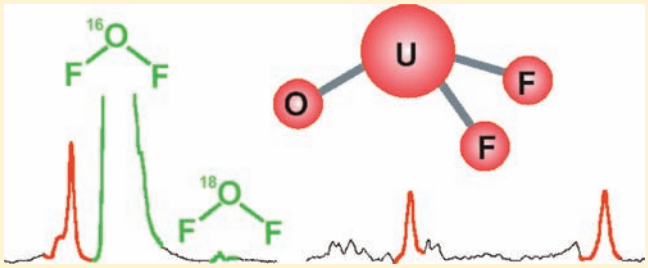

INTRODUCTION

Molecules with terminal metal oxo ligands are considered to be important intermediates in a number of chemical and biochemical reactions.[1−3] Considerable experimental effort has been devoted to the synthesis and characterization of these molecules especially those containing late transition metal centers, which are helpful in understanding their roles in the corresponding catalytic reactions.[4−7] Considering the importance of terminal oxo species in transition metal chemistry, their actinide analogues are also interesting because applications of uranium and thorium in a wide range of catalytic reactions have been the subject of much scientific research.[8−11] As the most widely studied actinide element, uranium is known to form a number of uranyl compounds containing UO_2^+ and UO_2^{2+} fragments, the structures of which have been fully characterized by experimental and theoretical methods.[12−15] Compared with the rich studies on these uranyl species containing uranium oxygen multiple bonds, molecules with terminal mono oxo groups are not as well structurally characterized,[16−18] which is partly related to their high reactivity toward the formation of bridged oxo species.[16] Although species like $UOCl_5^-$ and UOF_4 have also been characterized to have terminal UO groups in their solid states,[19,20] they have been classified as uranyl analogues because of preference for the almost linear X−U−Y arrangement around uranium,[16] where the inverse trans influence plays an important role.[13,21] For thorium, however, few structural reports can be found for molecules with terminal ThO groups.[22]

Besides experimental studies focused on synthetic methods, reactions of uranium and thorium atoms with simple precursor molecules in cryogenic matrixes have also yielded several products with terminal oxo ligands.[23−26] In these cases structural identification can be determined by the agreement of experimental and theoretical vibrational frequencies for a specific calculated structure. Our recent studies on actinide and NF_3 reaction products provided experimental evidence for the formation of terminal nitride species as the final products.[27,28] Hence, similar reaction product molecules with terminal oxo ligands are expected to be formed when OF_2 is used as the reactant, since the OF bond is even weaker than the NF bond in NF_3, and much weaker than the OH bond in H_2O.[23,29] In this paper, we report the matrix infrared spectra of two oxoactinide difluoride molecular species with terminal oxo groups, namely, OUF_2 and $OThF_2$. These product molecules are formed via the spontaneous, specific reactions of laser ablated uranium or thorium atoms and OF_2 in argon and neon matrixes. Three bond stretching mode absorptions are observed in the infrared above 400 cm^{-1} for each molecule, and they compare favorably with density functional calculations of vibrational frequencies. We also include a CASPT2 bonding

Received: May 4, 2012
Published: May 24, 2012

 © 2012 American Chemical Society dx.doi.org/10.1021/ic3009128 | *Inorg. Chem.* 2012, 51, 6983−6991

analysis which describes triple bonding in these early actinide oxo subunits.

EXPERIMENTAL AND THEORETICAL METHODS

The experimental apparatus and procedure for preparation and characterization of metal atom reaction product molecules in excess argon at 4 K have been described previously.[30] The Nd:YAG laser fundamental (1064 nm, 10 Hz repetition rate with 10 ns pulse width) was focused onto a freshly cleaned uranium or thorium (Oak Ridge National Laboratory, high purity) target mounted on a rotating rod. Laser-ablated uranium or thorium atoms were codeposited with 3−4 mmol of argon (Matheson, research) containing 1.0% OF_2 (Ozark-Mahoning) onto a CsI cryogenic window for 60 min. The $^{18}OF_2$ sample (91% ^{18}O enriched) was synthesized and kindly provided by Arkell and co-workers.[31] Both OF_2 and $^{18}OF_2$ samples were used without further purification in a stainless steel vacuum manifold. FTIR spectra were recorded at 0.5 cm^{-1} resolution and ±0.1 cm^{-1} frequency accuracy on a Nicolet 750 FTIR instrument with a HgCdTe range B detector. Matrix samples were annealed at different temperatures and cooled back to 4 K for spectral acquisition. Selected samples were subjected to broadband photolysis by a medium-pressure mercury arc street lamp (Philips, 175W) with the outer globe removed.

Complementary density functional theory (DFT) calculations were performed using the Gaussian 09 program system.[32] The hybrid B3LYP density functional was employed primarily in our calculations along with the M06 functional.[33] The 6-311+G(d) basis set was used for oxygen and fluorine atoms, and the 60 electron core SDD pseudopotentials were employed for thorium and uranium atoms.[34] All of the geometrical parameters were fully optimized, and the harmonic vibrational frequencies were obtained analytically at the optimized structures. The nature of the terminal oxo bonds in the OUF_2 and $OThF_2$ molecules were further analyzed using NBO 3.1 as implemented in Gaussian 09.[35] After the DFT work, benchmark CASPT2 calculations were done for OUF_2 [using (6,6) and (8/8) CAS] and for $OThF_2$ [(6,6) CAS].[36] The MOLPRO program package[36e] used for the latter calculations employs a slightly different code (RS2) and gives slightly different results from the MOLCAS program of Roos et al.

RESULTS AND DISCUSSION

Reactions of uranium or thorium atoms with OF_2 were studied using different OF_2 concentrations as well as laser energies, and only the best experimental results using 1.0% OF_2 are presented here. A common absorption due to the OF free radical was observed at 1028.1 cm^{-1} after sample deposition in all experiments,[37] and this absorption intensity depended strongly on the laser energy employed in the experiment. Broad band irradiation (λ > 220 nm) increased the intensity of the OF radical band, which decreased when the sample was annealed, as observed previously.[37c] In addition, weak absorptions for CF_4, CO, CO_2, O_3, and FOO[38] were also present in the matrix infrared spectra. Very weak CO and CO_2 contaminant absorptions are always observed in these experiments, and CF_4 is a common impurity in fluorine and OF_2 samples from the reactions of highly oxidative F_2 or OF_2 with residual carbon in the steel sample cylinders.

Infrared Spectra. Figure 1 shows infrared spectra from codeposition of laser-ablated uranium atoms with 1.0% OF_2 in argon. In addition to weak UO_2 and UO_2^+ absorptions as well as bands due to UF_x species,[39,40] several other new metal dependent (i.e., these bands depended on the particular metal source ablated) absorptions were observed after sample deposition. These were not present in U with O_2 or F_2 argon matrix experiments. Weak 940.5 and 871.7 cm^{-1} absorptions (not shown) were assigned to the antisymmetric O−U−O stretching modes of the UO_2F_2 and UO_2F molecules from

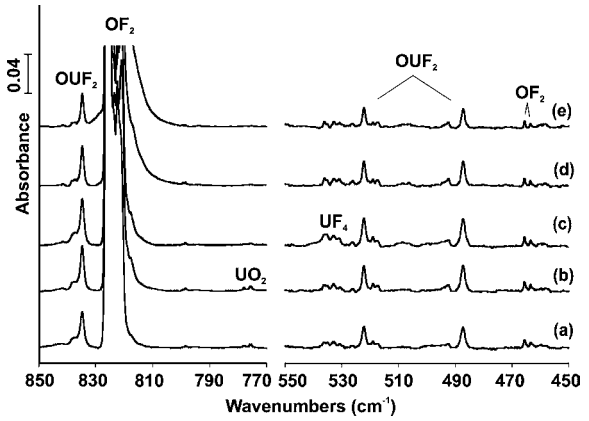

Figure 1. Infrared spectra of laser-ablated uranium atoms and OF_2 reaction products in solid argon at 4 K: (a) U + 1.0% OF_2 deposition for 60 min; (b) after annealing to 20 K; (c) after λ > 220 nm irradiation; (d) after annealing to 30 K; (e) after annealing to 35 K.

reactions of uranium with mixed F_2 and O_2 in argon.[41] New product bands were observed at 834.8, 522.2, and 487.2 cm^{-1}, which increased by ~10% during the first annealing to 20 K (Figure 1, trace b). Subsequent broad band irradiation had essentially no effect on these new bands while the uranium fluoride absorptions increased (Figure 1, trace c). Further sample annealing to 30 and 35 K decreased the 834.8, 522.2, and 487.2 cm^{-1} absorption set (Figure 1, traces d and e), and the UF_6 band at 619 cm^{-1} became the dominant absorption in the infrared spectra (not shown).[41] In addition, spectra are compared in Supporting Information, Figure S1 for U atom reaction products with OF_2 and with F_2.

Infrared spectra from the reactions of laser-ablated thorium atoms and OF_2 are shown in Figure 2. Weak absorptions

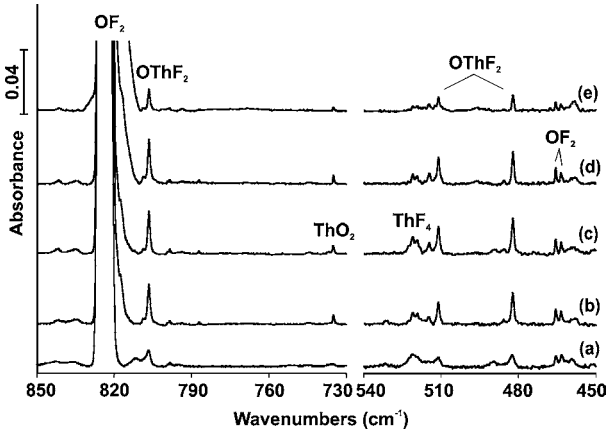

Figure 2. Infrared spectra of laser-ablated thorium atoms and OF_2 reaction products in solid argon at 4 K: (a) Th + 1.0% OF_2 deposition for 60 min; (b) after annealing to 20 K; (c) after λ > 220 nm irradiation; (d) after annealing to 30 K; (e) after annealing to 35 K.

previously assigned to ThO and ThO_2 molecules were observed right after sample deposition,[42] and their amounts are too small to observe any possible reaction products. Three new product absorptions at 806.6, 511.1, and 482.3 cm^{-1} increased substantially when the sample was annealed to 20 K because of the lower laser energy used for Th relative to that for U in the uranium experiments. But these bands decreased upon annealing to 30 and 35 K (Figure 2, traces b, d and e). No

dx.doi.org/10.1021/ic3009128 | Inorg. Chem. 2012, 51, 6983−6991

change was found for the 806.6, 511.1, and 482.3 cm^{-1} absorption set upon broad band irradiation while the ThF_4 absorption increased (Figure 2, trace c).[43] The latter two absorptions are clearly in the region for Th−F stretching vibrations.

To facilitate product identifications, experiments with $^{18}OF_2$ sample (91% enriched) were also carried out, which are diagnostic for identifying the UO and ThO stretching modes in the new molecules. Additionally, the metal fluoride stretching modes might also exhibit very small oxygen-18 shifts because of coupling with the metal oxide stretching modes. Infrared spectra from the reactions of uranium or thorium with 1.0% $^{18}OF_2$ in argon are shown in Figure 3 (traces c and d), and the newly observed product absorptions are listed in Table 1.

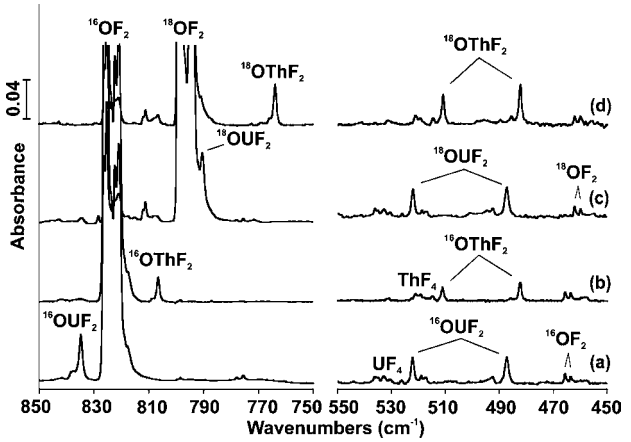

Figure 3. Infrared spectra of laser-ablated uranium and thorium atom and isotopically substituted OF_2 reaction products in solid argon at 4 K. All spectra were recorded after sample deposition followed by 20 K annealing: (a) U + 1.0% $^{16}OF_2$; (b) Th + 1.0% $^{16}OF_2$; (c) U + 1.0% $^{18}OF_2$ (91% enriched); (d) Th + 1.0% $^{18}OF_2$ (91% enriched).

Complementary neon matrix experiments were performed to ascertain the magnitude of the argon to neon matrix shifts and thus determine the influence of matrix atoms on the trapped species. The successful trapping of reactive molecules in solid neon made by reactions of laser ablated metal atoms necessitates lower laser energy and less heat load to the condensing sample because the 4 K substrate is much closer to the freezing point of neon (24.5 K) than that of argon (84.0 K). Hence, the product yield is typically less in the neon matrix, and such spectra are shown in Supporting Information, Figure S2 with the product absorptions given in Table 1. Absorptions due to uranium and thorium oxide molecules were observed as well.[42b,44] It is significant to note that these neon matrix counterparts are blue-shifted slightly more than the typical amount (here about 20 cm^{-1}) from the argon matrix values described above.[45] These argon−neon shifts can be compared to those observed for the CH_2-LnF_2 complexes in recent work from this laboratory.[46] Since the Ln-F bonds are almost purely ionic, the argon−neon matrix shifts are large (13−16 cm^{-1}) for the ionic Ln-F bond stretching modes and appropriately small (~1 cm^{-1}) for the more covalent Ln-C bond stretching modes. Hence, the argon−neon matrix shifts for the subject oxo species verify experimentally the polar character of these bonds which are revealed by the natural (NPA) atomic charges from the DFT calculations [O(−0.81) U(2.08) F(−0.63 × 2) and O(−1.03) Th(2.38) F (−0.68 × 2)] (see Supporting Information, Table S1).

The additional observation of the best yield of the UO diatomic molecule in solid neon here from the single oxygen OF_2 precursor at 899.2 cm^{-1} is in agreement with the earlier observation at 889.5 cm^{-1} from dioxygen reactions.[44] The $U^{18}O$ counterpart is observed here at 841.6 cm^{-1} with the $U^{16}O/U^{18}O$ frequency ratio of 1.05656. We maintain that UO is trapped in different electronic states in solid neon and solid argon where the vibrational mode absorption is 819.8 cm^{-1}.[39]

OMF_2 (M = U, Th) Molecules. The 834.8, 522.2, and 487.2 cm^{-1} absorptions exhibited identical behavior throughout the experiments with uranium, suggesting that they arise from different vibrational modes of the same new molecule. The 834.8 cm^{-1} band shifted to 790.5 cm^{-1} with the $^{16}O/^{18}O$ isotopic frequency ratio of 1.0560. Both the isotopic frequency ratio and band position (1.0571 and 819.8 cm^{-1} for UO in solid argon[39]) show that the 834.8 cm^{-1} band is due to the U−O stretching mode of a new molecule (the smaller 1.0529 isotopic frequency ratio is the signature of an antisymmetric O−U−O vibration.[39]). In addition the $^{18}OF_2$ sample contains 9% $^{16}OF_2$, and the relative intensities of the $^{16}OF_2$ and $^{18}OF_2$ isotopic products in the ^{18}O-enriched sample provide information on the oxygen stoichiometry of the new product: with a single O atom the relative 16/18 product band intensities would be (0.09)/(0.91) = 1/9, but with two O atoms, the relative 16,16/18,18 band intensities would be $(0.09)^2/(0.91)^2$ or 1/102. The measured integrated relative 16/18 uranium product band intensity is 1/5 where the ^{18}O-enriched product area is difficult to measure as a shoulder on the very intense $^{18}OF_2$ precursor band. However, the measured integrated relative 16/18 thorium product band intensity is 1/12 [here the ^{16}O-product

Table 1. Vibrational Frequencies Observed in Solid Argon and Solid Neon [in brackets] and Calculated Frequencies (Infrared Intensities) for the OUF_2 and $OThF_2$ Molecules Prepared from the $^{16}OF_2$ and $^{18}OF_2$ Reagents[a]

		$^{16}OF_2$		$^{18}OF_2$	
	mode	obsd.	calc.[b]	obsd.	calc.
OUF_2	U−O str.	834.8 [855.0]	862.4 (217)	790.5 [809.5]	816.3 (194)
	sym. F−U−F	522.2 [529.0]	521.3 (126)	522.1 [528.8]	521.2 (126)
	antisym. F−U−F	487.2 [507.6]	498.4 (185)	487.2 [507.6]	498.3 (184)
$OThF_2$	Th−O str.	806.6 [mask]	825.9 (235)	763.9 [782.7]	781.9 (209)
	sym. F−U−F	511.1 [522.4]	513.1 (126)	510.8 [522.0]	512.9 (127)
	antisym. F−U−F	482.3 [500.8]	484.6 (202)	482.1 [500.5]	484.5 (201)

[a]Only frequencies above 400 cm^{-1} are listed. Numbers in parentheses are infrared intensities (km/mol). [b]Our calculations employed the B3LYP density functional, and for comparison the M06 functional gave 859.2(260), 512.6 (129), and 483.8 (207) for $OThF_2$. Ref 47a gave 838.1 cm^{-1} (PBE) and 889.0 cm^{-1} (PBE0) for the U−O stretching mode of OUF_2 using SC-RECP basis set for uranium.

dx.doi.org/10.1021/ic3009128 | Inorg. Chem. 2012, 51, 6983−6991

intensity is from Figure 3 (spectrum d minus spectrum c) since the ^{18}O-enriched sample contains weak impurity bands in this region]. Both of these measured integrated relative 16/18 product band intensities are much closer to the 1/9 ratio expected for a single O atom containing product, in agreement with the isotopic frequency ratio and band position.

The new 522.2 and 487.2 cm^{-1} absorptions are observed in the region of uranium fluoride absorptions.[40] Experiments with $^{18}OF_2$ isotopic sample revealed that the former band red-shifted slightly to 522.1 cm^{-1} while no obvious isotopic shift was observed for the latter band. Since these two bands were not observed in the argon, U and F_2 experiments,[40] they are probably due to the uranium-fluoride stretching modes of the new oxygen containing molecule. Hence we assign the three new absorptions to the U−O stretching, symmetric and antisymmetric F−U−F stretching modes of the OUF_2 molecule. Note that the 834.8 cm^{-1} absorption corresponds to the weak 834.7 cm^{-1} band observed in previous argon matrix $U/O_2/F_2$ experiments, which was assigned incorrectly to the U−O stretching mode of the OUF_4 molecule as a minor product in those experiments.[41] However, as mentioned in that paper, it is not possible to distinguish unambiguously between the OUF_2 and the OUF_4 molecule possibilities based on observation of only the uranium-oxide stretching band without further experimental information like that provided here from the higher yield concerted U and OF_2 reaction. The observation of two additional uranium fluoride stretching modes along with the terminal U−O stretching mode in our new experiments validates the identification of OUF_2.

Assignments of the 806.6, 511.1, and 482.3 cm^{-1} absorptions to the $OThF_2$ molecule are straightforward following the uranium example. The 806.6 cm^{-1} band shifted to 790.5 cm^{-1} on oxygen-18 substitution, and the isotopic frequency ratio of 1.0559 for a typical Th−O stretching mode was observed for the 806.6 cm^{-1} band (1.0563 and 876.4 cm^{-1} for ThO in solid argon[42]). The 511.1 and 482.3 cm^{-1} absorptions due to symmetric and antisymmetric F−Th−F stretches exhibited 0.3 and 0.2 cm^{-1} red shifts upon ^{18}O substitution, which clearly demonstrates the slight involvement of oxygen in these two lower frequency vibrational modes.

To confirm further our experimental assignments and to get detailed insight into the structures of the product molecules, theoretical calculations using the B3LYP functional were carried out on the OUF_2 and $OThF_2$ molecules. The triplet state for OUF_2 is found to be lowest in energy while the $OThF_2$ molecule possesses a closed shell singlet ground state. The U−O stretching mode calculated for OUF_2 at 862.4 cm^{-1} shifts to 816.3 cm^{-1} with ^{18}O substitution, and the computed isotopic frequency ratio of 1.0565 is quite close to the experimental value of 1.0560. The other two vibrational frequencies above 400 cm^{-1} are predicted at 521.3 and 498.4 cm^{-1}, which are due to symmetric and antisymmetric F−U−F stretching modes, respectively. Note that the slight participation of oxygen in these two modes results in very small 0.1 cm^{-1} calculated ^{18}O shifts, which is in line with the negligible shifts observed experimentally (Table 1). Similar agreements are found between the calculated and observed frequencies for the $OThF_2$ molecule (Table 1). Both the calculated band position and $^{16}O/^{18}O$ isotopic frequency ratio for the Th−O stretching mode fit the experimental values well. The thorium fluoride stretching modes 0.2 and 0.1 cm^{-1} red shifts upon ^{18}O substitution as predicted by our calculations, which are also consistent with the observed shifts of 0.3 and 0.2 cm^{-1}.

B3LYP calculations were also performed on the OUF_4 molecule offered as a possible assignment in our earlier experiments.[41] Consistent with most previous investigations,[47] a C_{3v} structure is calculated to be most stable for the OUF_4 molecule. Frequency calculations reveal four infrared active modes above 400 cm^{-1}: the axial U−O and U−F stretches at 918.7 and 619.0 cm^{-1} as well as the equatorial U−F stretching modes at 554.6 and 533.6 cm^{-1} with relative intensities of 160:87:432:20. Clearly, assignment of the new 834.8, 522.2, and 487.2 cm^{-1} absorptions to the OUF_4 molecule is not a reasonable possibility.

Structure and Bonding. Geometry optimizations on the OUF_2 and $OThF_2$ molecules give pyramidal structures (Figure 4). These are related to other OUX_2 and $OThX_2$ species (X = H, CH_3) identified in earlier matrix isolation experiments,[23−26] where the geometries are believed to involve 6d orbitals as exemplified in the H_2ThO molecule.[24] The U−O bond length of the OUF_2 molecule is calculated here by B3LYP to be 1.830 Å, almost the same as that for $OU(CH_3)_2$ (1.833 Å) and OUH_2 (1.823 Å) at the same level of theory.[26] This is in line with the small changes in the U−O stretching frequencies for these molecules.[23,26] A similar trend is found for $OThF_2$ frequencies and its analogues.[24,26]

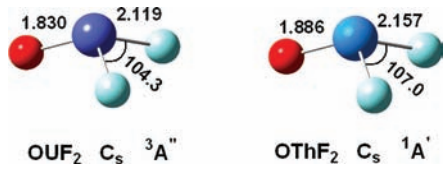

Figure 4. Optimized structures (bond lengths in angstroms and bond angles in degree) for the OUF_2 and $OThF_2$ molecules at the B3LYP/6-311+G(d) level of theory. Structural parameters were almost the same with those given in ref. 47a. Structural parameters are also similar using the CASPT2 method (Supporting Information, Table S1).

Selected molecular orbitals for OUF_2 from B3LYP calculations are shown in Supporting Information, Figure S3 so as to understand better the multiple bonding interactions involved in this molecule. The two unpaired electrons are left in the highest occupied molecular orbital (HOMO) and HOMO-1, which are mostly U 5f orbital in character. The HOMO-2 is apparently a σ bonding orbital formed mainly via the U 6d and O 2p interactions. Both HOMO-3 and HOMO-4 are π bonding orbitals arising from the overlap between oxygen 2p lone pair and uranium 6d orbitals with the former contributing more. Calculations reveal that the U−O bond distance in the OUF_2 molecule is 1.830 Å at the B3LYP level, 1.8312 Å with CASPT2 (6,6), and 1.8314 Å using the (8,8) active space (Supporting Information, Table S1), which are close to the values of recently characterized terminal uranium oxo complexes.[16,17,48] The size of the (6,6) active space is in principle large enough because of the mostly ionic U−F bonds formed. Therefore, one only needs six active orbitals with six electrons to describe the multiple bonding character of the O−U bond.

The computed U−O bond distance in the OUF_2 molecule is 0.12 Å longer than the tabulated UO triple bond length proposed from triple bond radii,[49a] but near the experimental bond length for UO (1.838 Å).[49b] However, this proposed triple bond radius is based on the *uranyl dipositive cation*, which clearly has shorter bond lengths than a neutral species, and is not a good comparison for multiple bond lengths in neutral

dx.doi.org/10.1021/ic3009128 | *Inorg. Chem.* 2012, 51, 6983−6991

species. Hence, the UO bond in our OUF_2 molecule has considerable triple bond character, the same as suggested for other terminal UO containing species.[47,48] The OUF_2 molecule can be compared with the isostructural OUH_2 molecule.[23] The computed dipole moment of the former is 5.61 D, and the Mulliken atomic charges are O(−0.63) U(1.60) F_2(−0.49)$_2$ and of the latter is 5.17 D with Mulliken atomic charges of O(−0.58) U(1.22) H_2(−0.32)$_2$.

Additional support for the multiple bonding in the OUF_2 molecule can be obtained from natural bond orbital (NBO) analysis.[35] As shown in Table 2, three U−O bonding orbitals

Table 2. Composition of the Bonding Molecular Orbitals in the OUF_2 and $OThF_2$ Molecules from NBO Calculations[a]

			metal atomic orbital content in this bond,%			
	bond type	% of the NBO on each atom	s	p	d	f
OUF_2	π	O (80.42)	1.85	98.10	0.05	
		(83.85)	**1.48**	**98.48**	**0.05**	
		U (19.58)	0.32	0.82	48.62	50.23
		(16.15)	**0.26**	**0.85**	**53.06**	**45.83**
	π	O (82.00)	0	99.95	0.05	
		(84.87)	**0**	**99.95**	**0.05**	
		U (18.00)	0	1.47	47.23	51.30
		(15.13)	**0**	**1.51**	**47.01**	**51.48**
	σ	O (75.58)	13.04	86.91	0.04	
		(78.72)	**17.30**	**82.66**	**0.04**	
		U (24.42)	0.49	2.47	46.67	50.37
		(21.28)	**0.71**	**3.00**	**55.21**	**41.09**
$OThF_2$	π	O (85.00)	0.69	99.27	0.04	
		Th (15.00)	1.55	2.23	61.10	35.12
	σ	O (82.01)	16.84	83.13	0.02	
		Th (17.99)	0.23	4.35	56.21	39.20
	π	O (86.67)	0	99.96	0.04	
		Th (13.33)	0	2.08	56.73	41.20

[a]Numbers in bold type are for β spin orbitals in $^3A''$ OUF_2.

are found, in which the oxygen atom (mainly 2p orbital) contributes about 80% to the U−O bond while the remaining 20% contributions come from the equivalent hybridization of U 6d and 5f orbitals. This contrasts the bonding situation in the Cp_2UO molecule, which is considered to be $Cp_2U^{(+)}$-$O^{(-)}$ with a U−O single bond because of the localized nature of the six electrons on oxygen.[50] Similar with the triple U−O bond in the OUF_2 molecule, the U−O σ bond in the Cp_2UO molecule also contains 80% oxygen participation. The natural charge on the uranium center in the Cp_2UO molecule is +2.49,[50] which is higher than our value for OUF_2 (+2.11) and consistent with more covalent character in the latter molecule. Since fluorine is highly electronegative, it is expected that the electrons on oxygen tend to overlap more with the uranium orbitals, which is different from the case with the cyclopentadienyl ligand.

The B3LYP computed bond order of 2.95 for OUF_2 from NBO analysis also supports the triple bond character for the terminal oxo bond. For comparison, similar calculations for quintet UO at the B3LYP level of approximation gave a 2.97 bond order. To confirm this oxo bonding scheme, benchmark level CASPT2 level calculations were done, which have been used to describe multiple bonding in a number of simple uranium bearing species including NUF_3.[27] The CASPT2 molecular orbitals shown in Figure 5 reveal a bond order of

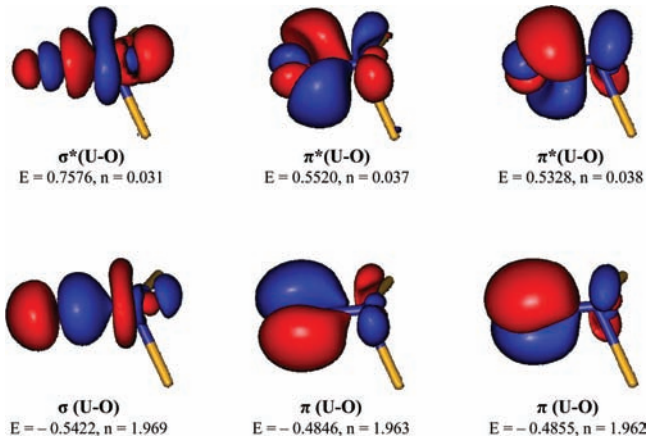

Figure 5. CASPT2-Molecular orbitals for the oxo bond in OUF_2.

2.894, which characterizes a triple oxo bond in OUF_2. Since additional π bonding comes from dative electron donation from oxygen, while the unpaired electrons of uranium occupy the two f orbitals, the formal oxidation state of uranium is still best described as IV. The singly occupied CASPT2 f orbitals are illustrated in Supporting Information, Figure S4.

The bonding interactions in the singlet $OThF_2$ molecule are very similar to those for OUF_2 except that the Th−F bond is more ionic. It is also reasonable to consider triple bond character for the ThO bond in the $OThF_2$ molecule with the existence of one σ and two π bonds, the latter of which can be mainly viewed as dative bonds with lone pair electron densitiy donated from the oxygen center. The Th−O distance (1.886 Å) in the $OThF_2$ molecule is also consistent with the value for the recently characterized thorium oxo metallocenes (1.929 Å),[22] and almost the same as the ThO triple bond length (1.89 Å) taken from atomic radii,[49a] but longer than the measured bond length for ThO ($^1\Sigma^+$) itself (1.840 Å).[49c] The B3LYP calculated bond length is 1.835 Å, and the harmonic frequency is 896.1 cm^{-1} (224 km/mol intensity) for ThO.[41b] As can be found in Table 2, the Th−O bond is a triple bond as well because of the three bonding orbitals in spite of the slightly larger participation of oxygen 2p orbitals, which is similar with the uranium case. The natural charge on the thorium center is +2.38, slightly higher than the charge on uranium. This is consistent with the lesser contribution from thorium to the Th−O bond, giving rise to a more ionic character. The triple bond character for the terminal oxo ligand in $OThF_2$ is also supported by the B3LYP NBO calculated bond order of 2.94, close to the value of 2.96 computed here for the ThO diatomic molecule. Additionally, the Th 5f orbitals are found to be involved in the Th−O bonding from NBO analysis, although Th does not have 5f valence electrons. In conclusion, the ThO bond in the $OThF_2$ molecule also has considerable triple bond character, which is illustrated nicely by the CASPT2 molecular orbitals, Figure 6, and the computed 2.892 bond order.

Our recent studies identified the CH_2UF_2 molecule, which is isoelectronic with the OUF_2 molecule.[51] The CH_2UF_2 molecule is predicted to have some CH-U agostic interaction with the uranium center in a pyramidal geometry. Although one of the fluoride stretching modes of the CH_2UF_2 molecule was not resolved, the symmetric and antisymmetric F−U−F stretching vibrational frequencies of the CD_2UF_2 methylidene were observed at 528.3 and 507.4 cm^{-1}, only 6 and 20 cm^{-1} higher than those of the OUF_2 molecule. For the CH_2ThF_2

dx.doi.org/10.1021/ic3009128 | Inorg. Chem. 2012, 51, 6983−6991

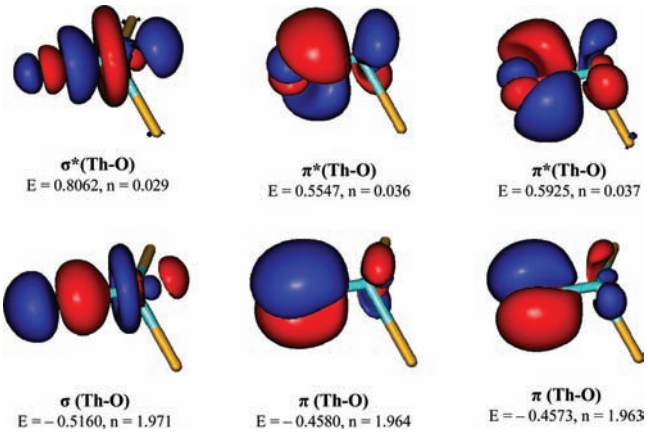

Figure 6. CASPT2-Molecular orbitals for the oxo bond in $OThF_2$.

molecule, an approximately symmetrical structure was found by the B3LYP functional, and it also showed a slightly pyramidal geometry around Th.[52] Compared with the fluoride stretching frequencies of $OThF_2$, the symmetric stretching mode of the CH_2ThF_2 methylidene complex was almost the same, but the antisymmetric mode was about 15 cm^{-1} higher, which agree with the small changes in bond lengths. In addition to the methylidene complexes, the first actinide borylene complex, $FBThF_2$, was recently identified in solid argon from the reactions of BF_3 and thorium.[53] Since only three valence electrons are available for boron, the FB fragment can only form one σ and one π bond with the corresponding thorium orbitals, which results in a Th═B double bond. To further compare the geometric changes for the $XThF_2$ (X = BF, CH_2, O) molecules, the structural parameters of the CH_2ThF_2 and $OThF_2$ molecules were optimized using the B3LYP functional and the larger 6-311+G(3df) basis set, which is the same as the one used for $FBThF_2$. The changes in Th−F bond lengths are within 0.01 Å and the changes in bond angles are less than 2 degrees compared with the results using the smaller 6-311+G(d) basis set. The borylene $FBThF_2$ still possesses the shortest computed Th−F bond (2.119 Å) followed by CH_2ThF_2 (2.129 Å) and $OThF_2$ (2.147 Å), which is also consistent with its highest fluoride stretching frequencies observed near 540 and 525 cm^{-1},[53] about 30 and 40 cm^{-1} higher than those of the $OThF_2$ molecule. The calculated FThF bond angle for $FBThF_2$ is 126.9°, larger than that for CH_2ThF_2 (120.6°) and $OThF_2$ (106.5°) all calculated with large basis sets while the difference in XThF bond angle is smaller with $OThF_2$ (112.3°) followed by $FBThF_2$ (108.5°) and CH_2ThF_2 (106.5°). It is interesting to note that the in-plane π bonding orbital for the CH_2ThF_2 molecule is mainly a Th−C nonbonding orbital, but it has some C−H bonding character, which is obviously different from the in-plane π bonding orbital for $OThF_2$ (Figure 7). This results in a true Th═C double bond for the CH_2ThF_2 molecule. In the case of $FBThF_2$, only one σ and one out-of-plane π orbital were found while the in-plane orbital does not exist because of only three valence electrons for boron. As a result, the FThF bond angle is larger when the ThX bond involves in-plane π interaction, the presence of which is believed to increase the repulsive interactions between terminal Th−F σ bond and this π bond. Hence, the FThF bond angles are sensitive to the existence of the second π bonding orbital in such a system with multiple ThX bonds.

OUF_2/$OThF_2$ in the Condensed Phase. Both uranium and thorium oxyfluorides have been reported in the solid state

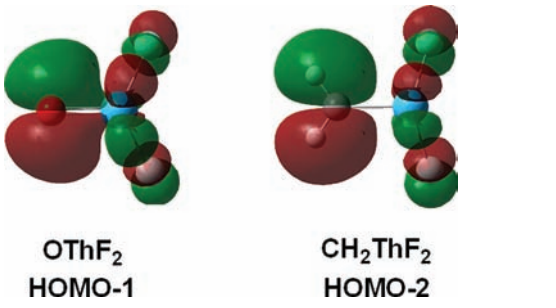

Figure 7. In-plane π orbitals for the isoelectronic $OThF_2$ and CH_2ThF_2 molecules.

several decades ago. The uranium oxide tetrafluoride compound (UOF_4) was characterized to have axial fluorine and oxygen atoms with four bridged and one nonbridged equatorial fluorine atom around the uranium center.[20] The presence of nonbridged oxygen atom was supported by the observation of a strong presumably U−O stretching band at 885−881 cm^{-1}, the absence of bridged UOU stretching modes, as well as structural parameters determined by neutron diffraction, which showed a UO distance of 1.870 Å.[54] This is slightly longer than the UO bond length computed for the OUF_2 molecule (1.830 Å) and several structurally characterized terminal UO containing compounds.[16−18]

The existence of the OUF_2 compound has been proposed in its water complex $OUF_2{\cdot}H_2O$ without direct structural information.[55] However, all of the heavier analogues, OUX_2 (X = Cl, Br, I), have been characterized to have bridged oxo structures.[56,57] Similarly, structural studies on the thorium oxyfluorides ($OThF_2$) as well as other oxyhalides suggested that only bridged oxygen atoms are present in these solid compounds, which possess longer ThO distances as well as bridged ThOTh vibrational modes.[57−59]

Several aspects of the solution chemistry of the OUF_2 molecule are noteworthy.[55] As the pH is increased to 1.7, the color changes from green to blue to brown and ultimately a black precipitate is formed. This black material was found to be 76.25% U by mass, which suggested the stoichiometry $(UF_2)(OH)_2$ or $(OUF_2)(H_2O)$. The NMR spectrum of this material is sharp compared to that of $(UF_4)(H_2O)_{1.5,\ 2.5}$, which suggested that the H_2O ligand in the $(OUF_2)(H_2O)$ complex is mobile in solution. We suspect a dipole bound complex for the two polar molecules OUF_2 and H_2O, with computed dipole moments of 5.61 and 2.16 D, respectively (The experimental value for H_2O is 1.854 D, and our B3LYP value is 20% higher.).[60] Accordingly, B3LYP calculations were done for this complex, the structure is illustrated in Supporting Information, Figure S5, and its chemistry is discussed in our Supporting Information.

Reactions in the Matrix. As shown in Figures 1 and 2, ground state uranium and thorium atoms react with OF_2 on low temperature annealing in solid argon, which results in the spontaneous formation of the OUF_2 and $OThF_2$ molecules. No $M(OF_2)$ complexes nor FOMF (M = U,Th) insertion product intermediates were observed in our experiments. Our B3LYP calculations reveal that geometry optimizations of the $M(OF_2)$ and FOMF molecules (quintet for U, triplet and singlet for Th) give rise to the OMF_2 structures, suggesting that neither $M(OF_2)$ nor FOMF is stable along the reaction coordinates of uranium and thorium with OF_2. Since both Th−F and U−F bonds are about three times as strong as the O−F bond,[29,61,62]

dx.doi.org/10.1021/ic3009128 | Inorg. Chem. 2012, 51, 6983−6991

formation of the OUF_2 and $OThF_2$ molecules is expected to be highly exothermic, and these molecules are further stabilized through triple bonds in the UO and ThO linkages. Our B3LYP calculations reveal that the bond dissociation energies for the U−F and Th−F bonds in the OMF_2 molecules are 137 and 143 kcal/mol, while those for the U−O and Th−O bonds are 160 and 185 kcal/mol. The overall reaction exothermicites for the formation of the OUF_2 and $OThF_2$ molecules are quite large, 377 and 419 kcal/mol, respectively, for reactions 1 and 2, computed at the B3LYP level of theory without spin orbit corrections. Although no UO was detected in the argon matrix experiments, $U^{16}O$ is masked by the intense OF_2 absorption and weak $U^{16}O_2$ bands may cover any weak $U^{18}O$ absorption.[39] However, UO was observed in the neon matrix experiment, which may arise from the slower condensation and relaxation rate of energized product molecules formed in neon freezing at 4 K.

$$U + OF_2 \rightarrow OUF_2 \quad (1)$$

$$Th + OF_2 \rightarrow OThF_2 \quad (2)$$

A series of recent investigations on the reactions of fluorine substituted molecules with uranium and thorium has demonstrated that molecules containing as many metal fluorine bonds as possible were usually the final observed products.[27,28,51,52,63,64] This leads to the formation of a series of uranium carbide and nitride molecules as well as the terminal oxo species with multiple bonds identified here.[27,64] Formation of the $FC{\div}ThF_3$ and $N{\div}ThF_3$ molecules with two singly occupied π bonds was still favorable[28,52] even if the C−F bond is stronger than the N−F bond.[29] However the strongest B−F bond makes the BF_3 and thorium reactions terminate at the borylene complex $FBThF_2$ without further fluorine transfer to give the $B{\div}ThF_3$ molecule.[53]

OF_2 is known to decompose upon absorbing UV photons.[65] As a result, photodecomposition of OF_2 is expected during sample deposition due to irradiation from the plume produced by laser ablation of metal target, which contains UV and vacuum UV photons.[66] The intensity of the plume radiation can be changed by the laser energy, which accounts for the laser energy dependence of the OF band intensity. A similar process occurs when the sample is exposed to UV irradiation, both here and in earlier work, where Arkell et al. first prepared OF.[65] Along with the decomposition of OF_2, the OF radical band appeared. Additionally, atomic fluorine and oxygen were produced at the same time, which were evidenced by the presence of metal fluoride as well as weak ozone absorptions.

Previous studies on the reactions of uranium with F_2 and O_2 mixtures suggested that the UO_2F_2 and UO_2F molecules were major products while a weak band due to a single oxygen containing species was detected.[41] Uranium fluoride absorptions especially UF_6 became dominant when more concentrated fluorine samples were used. In contrast, the dioxo uranium fluoride species were stronger in the experiments with more O_2, which favors the formation of uranium dioxide as well as its fluorine adducts. In the case of OF_2, the fluorine transfer reactions make it possible for the formation of the molecules with one oxygen atom, and the fluoro and dioxo species are weak. Finally, these matrix reactions can be used to make an interesting series of metal containing molecules with terminal oxo groups.

CONCLUSIONS

Reactions of laser ablated uranium and thorium atoms with OF_2 have been investigated using matrix isolation infrared spectroscopy. Uranium and thorium oxyfluoride species, OUF_2 and $OThF_2$, are identified by the observations of terminal M-O and two F−M−F (M = U, Th) stretching vibrational modes as well as density functional vibrational frequency calculations. The OUF_2 and $OThF_2$ molecules are produced via the reactions of uranium and thorium atoms with OF_2 upon sample annealing, during which negligible activation energy is required. This is the first example of an oxide-fluoride molecule prepared in a single concerted reaction. All aspects of uranium-fluorine chemistry are important: first, for the investigation of chemical bonding, and second, for better understanding of applications for uranium fluorides such as the well-known separation of U isotopes through the diffusion of UF_6 isotopomers.

B3LYP and CASPT2 calculations predict pyramidal structures for these two oxyfluoride products. The closed shell singlet is found to be the ground state for the thorium product while triplet OUF_2 is calculated to be lowest in energy. Bonding analysis (NBO) reveals that the UO and ThO fragments in OUF_2 and $OThF_2$ contain considerable triple bond character because of the existence of an in-plane π bond, which is also reflected in the F−M−F bond angles as compared to molecules with similar structures. Benchmark CASPT2 calculations reveal 2.9 bond orders for each of these new oxo species and demonstrate the importance of dative bonding involving $O_{2p} \rightarrow Th_{6d}$ and U_{6d5f} interactions. The highly exothermic character of the OF_2 reactions suggest that numerous metal containing species with terminal oxo groups can be prepared using these fluorine transfer reactions.

ASSOCIATED CONTENT

Supporting Information

Complete references 32 and 36e, computed data table, comparison of U and OF_2 vs F_2 reaction product argon matrix infrared spectra, and neon matrix spectra for Th and U vs OF_2 reaction products. This material is available free of charge via the Internet at http://pubs.acs.org.

AUTHOR INFORMATION

Corresponding Author

*E-mail: lsa@virginia.edu.

Notes

The authors declare no competing financial interest.

ACKNOWLEDGMENTS

We gratefully acknowledge financial support from DOE Grant DE-SC0001034 and NCSA computing Grant CHE07-0004N. We thank Al Arkell of Texaco Research for the enriched $^{18}OF_2$ sample and our colleague Sergei Egorov for translation and helpful discussion of the work in ref 55. We appreciate Bjorn Roos for his many contributions to our understanding of chemical bonding. S.R. and T.S. gratefully acknowledge financial support from Fonds der Chemischen Industrie (FCI). The authors are grateful to the BWGrid cluster for providing computational resources.

REFERENCES

(1) Nugent, W. A.; Mayer, J. M. *Metal-Ligand Multiple Bonds*; Wiley: New York, 1988.

(2) (a) Nam, W. *Acc. Chem. Res.* **2007**, *40*, 522−531. (b) Yoshizawa, K. *Acc. Chem. Res.* **2006**, *39*, 375−382. (c) Gunay, A.; Theopold, K. H. *Chem. Rev.* **2010**, *110*, 1060−1081.
(3) Somorjai, G. A. *Introduction to Surface Chemistry and Catalysis*; Wiley: New York, 1994.
(4) Rohde, J. U.; In, J. H.; Lim, M. H.; Brennessel, W. W.; Bukowski, M. R.; Stubna, A.; Münck, E.; Nam, W.; Que, L., Jr. *Science* **2003**, *299*, 1037−1039.
(5) Poverenov, E.; Efremenko, I.; Frenkel, A. I.; Ben-David, Y.; Shimon, L. J. W.; Leitus, G.; Konstantinovski, L.; Martin, J. M. L.; Milstein, D. *Nature* **2008**, *455*, 1093−1096.
(6) (a) Anderson, T. M.; Neiwert, W. A.; Kirk, M. L.; Piccoli, P. M. B.; Schultz, A. J.; Koetzle, T. F.; Musaev, D. G.; Morokuma, K.; Cao, R.; Hill, C. L. *Science* **2004**, *306*, 2074−2077. (b) Anderson, T. M.; Cao, R.; Slonkina, E.; Hedman, B.; Hodgson, K. O.; Hardcastle, K. I.; Neiwert, W. A.; Wu, S.; Kirk, M. L.; Knottenbelt, S.; Depperman, E. C.; Keita, B.; Nadjo, L.; Musaev, D. G.; Morokuma, K.; Hill, C. L. *J. Am. Chem. Soc.* **2005**, *127*, 11948−11949. (c) Cao, R.; Anderson, T. M.; Piccoli, P. M. B.; Schultz, A. J.; Koetzle, T. F.; Geletii, Y. V.; Slonkina, E.; Hedman, B.; Hodgson, K. O.; Hardcastle, K. I.; Fang, X.; Kirk, M. L.; Knottenbelt,; Kögerler, P.; Musaev, D. G.; Morokuma, K.; Takahashi, M.; Hill, C. L. *J. Am. Chem. Soc.* **2007**, *129*, 11118−11133.
(7) Saouma, C. T.; Peters, J. C. *Coord. Chem. Rev.* **2011**, *255*, 920−937.
(8) Arnold, P. L. *Chem. Commun.* **2011**, *47*, 9005−9010.
(9) Fox, A. R.; Bart, S. C.; Meyer, K.; Cummins, C. C. *Nature* **2008**, *455*, 341−349.
(10) Andrea, T.; Eisen, M. S. *Chem. Soc. Rev.* **2008**, *37*, 550−567.
(11) Barnea, E.; Eisen, M. S. *Coord. Chem. Rev.* **2006**, *250*, 855−899.
(12) Fortier, S.; Hayton, T. W. *Coord. Chem. Rev.* **2010**, *254*, 197−214.
(13) Denning, R. G. *J. Phys. Chem. A* **2007**, *111*, 4125−4143.
(14) Arnold, P. L.; Love, J. B.; Patel, D. *Coord. Chem. Rev.* **2009**, *253*, 1973−1978.
(15) Graves, C. R.; Kiplinger, J. L. *Chem. Commun.* **2009**, 3831−3853.
(16) Hayton, T. W. *Dalton Trans.* **2010**, *39*, 1145−1158.
(17) (a) Fortier, S.; Kaltsoyannis, N.; Wu, G.; Hayton, T. W. *J. Am. Chem. Soc.* **2011**, *133*, 14224−14227. (b) Fortier, S.; Brown, J. L.; Kaltsoyannis, N.; Wu, G.; Hayton, T. W. *Inorg. Chem.* **2012**, *51*, 1625−1633.
(18) (a) Kraft, S. J.; Walensky, J.; Fanwick, P. E.; Hall, M. B.; Bart, S. C. *Inorg. Chem.* **2010**, *49*, 7620−7622. (b) Evans, W. J.; Kozimor, S. A.; Ziller, J. W. *Polyhedron* **2004**, *23*, 2689−2694.
(19) de Wet, J. F.; du Preez, J. G. H. *J. Chem. Soc., Dalton Trans.* **1978**, 592−597.
(20) Paine, R. T.; Ryan, R. R.; Asprey, L. B. *Inorg. Chem.* **1975**, *14*, 1113−1117.
(21) (a) Denning, R. G. *Struct. Bonding (Berlin)* **1992**, *79*, 215−276. (b) Kaltsoyannis, N. *Chem. Soc. Rev.* **2003**, *32*, 9−16.
(22) Ren, W. S.; Zi, G. F.; Fang, D. C.; Walter, M. D. *J. Am. Chem. Soc.* **2011**, *133*, 13183−13196.
(23) Liang, B.; Hunt, R. D.; Kushto, G. P.; Andrews, L.; Li, J.; Bursten, B. E. *Inorg. Chem.* **2005**, *44*, 2159−2168.
(24) Liang, B.; Andrews, L.; Li, J.; Bursten, B. E. *J. Am. Chem. Soc.* **2002**, *124*, 6723−6733.
(25) Gong, Y.; Andrews, L. *Inorg. Chem.* **2011**, *50*, 7099−7105.
(26) Gong, Y.; Andrews, L. *Dalton Trans.* **2011**, *40*, 11106−11114.
(27) Andrews, L.; Wang, X. F.; Lindh, R.; Roos, B. O.; Marsden, C. J. *Angew. Chem., Int. Ed.* **2008**, *47*, 5366−5370.
(28) Wang, X. F.; Andrews, L. *Dalton Trans.* **2009**, 9260−9265.
(29) CRC *Handbook of Chemistry and Physics*; CRC Press: Boca Raton, FL, 1985−1986.
(30) (a) Andrews, L.; Citra, A. *Chem. Rev.* **2002**, *102*, 885−911. (b) Andrews, L. *Chem. Soc.Rev.* **2004**, *33*, 123−132.
(31) Reinhard, R. R.; Arkell, A. *Int. J. Appl. Radiat. Isot.* **1965**, *16*, 498−499.
(32) Frisch, M. J.; et al. *Gaussian 09*, Revision B.01; Gaussian, Inc.: Wallingford, CT, 2010.
(33) (a) Becke, A. D. *J. Chem. Phys.* **1993**, *98*, 5648−5652. (b) Lee, C.; Yang, W.; Parr, R. G. *Phys. Rev. B* **1988**, *37*, 785−789.
(34) (a) McLean, A. D.; Chandler, G. S. *J. Chem. Phys.* **1980**, *72*, 5639−5648. (b) Krishnan, R.; Binkley, J. S.; Seeger, R.; Pople, J. A. *J. Chem. Phys.* **1980**, *72*, 650−654. (c) Kuchle, W.; Dolg, M.; Stoll, H.; Preuss, H. *J. Chem. Phys.* **1994**, *100*, 7535−7542.
(35) Reed, A. E.; Curtiss, L. A.; Weinhold, F. *Chem. Rev.* **1988**, *88*, 899 , and references therein..
(36) (a) Roos, B. O. The Complete Active Space Self-Consistent Field Method and its Applications in Electronic Structure Calculations. In *Advances in Chemical Physics; Ab Initio Methods in Quantum Chemistry − II*; Lawley, K. P., Ed.; John Wiley & Sons Ltd.: New York, 1987; Chapter 69, p 399. (b) Andersson, K.; Malmqvist, P.-Å.; Roos, B. O. *J. Chem. Phys.* **1992**, *96*, 1218. (c) Roos, B. O.; Lindh, R.; Malmqvist, P.-Å.; Veryazov, V.; Widmark, P.-O. *J. Phys. Chem. A* **2005**, *109*, 6575 ANO-RCC-VTZP basis. (d) Karlström, G.; Lindh, R.; Malmqvist, P.-Å.; Roos, B. O.; Ryde, U.; Veryazov, V.; Widmark, P.-O.; Cossi, M.; Schimmelpfennig, B.; Neograday, P.; Seijo, L. *Comput. Mater. Sci.* **2003**, *28*, 222. (e) Werner, H.-J.; Knowles, P. J. et al. *MOLPRO*, 2006.1 ed.; University of Birmingham: Birmingham, U.K., 2006.
(37) (a) Andrews, L. *J. Chem. Phys.* **1972**, *57*, 51−55. (b) Andrews, L.; Raymond, J. I. *J. Chem. Phys.* **1971**, *55*, 3078−3086. (c) Arkell, A. *J. Am. Chem. Soc.* **1965**, *87*, 4057−4062.
(38) Jacox, M. E. *J. Mol. Spectrosc.* **1980**, *84*, 74−88.
(39) Hunt, R. D.; Andrews, L. *J. Chem. Phys.* **1993**, *98*, 3690−3696.
(40) Hunt, R. D.; Thompson, C.; Hassanzadeh, P.; Andrews, L. *Inorg. Chem.* **1994**, *33*, 388−391.
(41) Souter, P. F.; Andrews, L. *J. Mol. Struct.* **1997**, *412*, 161−167.
(42) (a) Gabelnick, S. D.; Reedy, G. T.; Chasanov, M. G. *J. Chem. Phys.* **1974**, *60*, 1167−1171. (b) Andrews, L.; Gong, Y.; Liang, B.; Jackson, V. E.; Flamerich, R.; Li, S.; Dixon, D. A. *J. Phys. Chem. A* **2011**, *115*, 14407−14416.
(43) (a) Buchmarina, V. N.; Gerasimov, A. Y.; Predtechenskii, Y. B.; Shklyarik, V. G. *Opt. Spektrosk. (USSR)* **1992**, *72*, 69−74. (b) unpublished infrared spectra from this laboratory of Th reaction products with F_2 in excess argon at 4 K.
(44) Zhou, M. F.; Andrews, L.; Ismail, N.; Marsden, C. *J. Phys. Chem. A* **2000**, *104*, 5495−5502.
(45) Jacox, M. E. *Chem. Phys.* **1994**, *189*, 149−159.
(46) Wang, X. F.; Cho, H. G.; Andrews, L.; Chen, M. Y.; Dixon, D. A.; Hu, H. S.; Li, J. *J. Phys. Chem. A* **2011**, *115*, 1913−1921.
(47) (a) Shamov, G. A.; Schreckenbach, G.; Vo, T. N. *Chem.—Eur. J.* **2007**, *13*, 4932−4947. (b) Kovács, A.; Konings, R. J. M. *ChemPhysChem* **2006**, *7*, 455−462.
(48) (a) Bart, S. C.; Anthon, C.; Heinemann, F. W.; Bill, E.; Edelstein, N. M.; Meyer, K. *J. Am. Chem. Soc.* **2008**, *130*, 12536−12546. (b) Kosog, B.; La Pierre, H. S.; Heinemann, F. W.; Liddle, S. T.; Meyer, K. *J. Am. Chem. Soc.* **2012**, *134*, 5284−5289.
(49) (a) Pyykkö, P.; Riedel, S.; Patzschke, M. *Chem.—Eur. J.* **2005**, *11*, 3511−3520. (b) Heaven, M. C. *Phys. Chem. Chem. Phys.* **2006**, *8*, 4497−4509. (c) Huber, K. P.; Herzberg, G. *Molecular Spectra and Molecular Structure of Diatomic Molecules*; Van Nostrand: New York, 1979.
(50) (a) Zi, G.; Jia, L.; Werkema, E. L.; Walter, M. D.; Gottfriedsen, J. P.; Andersen, R. A. *Organometallics* **2005**, *24*, 4251−4264. (b) Barros, N.; Maynau, D.; Maron, L.; Eisenstein, O.; Zi, G.; Andersen, R. A. *Organometallics* **2007**, *26*, 5059−5065.
(51) Lyon, J. T.; Andrews, L.; Hu, H. S.; Li, J. *Inorg. Chem.* **2008**, *47*, 1435−1442.
(52) Lyon, J. T.; Andrews, L. *Eur. J. Inorg. Chem.* **2008**, 1047−1058.
(53) Wang, X. F.; Roos, B. O.; Andrews, L. *Chem. Commun.* **2010**, *46*, 1646−1648.
(54) Levy, J. H.; Taylor, J. C.; Wilson, P. W. *J. Inorg. Nucl. Chem* **1977**, *39*, 1989−1991.
(55) Vdovenko, V. M.; Romanov, G. A.; Solntseva, L. V. *Radiokhimiya* **1967**, *9*, 727−729.
(56) Levet, J. C.; Noël, H. *J. Solid State Chem.* **1979**, *28*, 67−73.
(57) Bagnall, K. W.; Brown, D.; Easey, J. F. *J. Chem. Soc. A* **1968**, 288−291.

(58) D'Eye, R. W. M. *J. Chem. Soc.* **1958**, 196−199.
(59) Scaife, D. E.; Turnbull, A. G.; Wylie, A. W. *J. Chem. Soc.* **1965**, 1432−1437.
(60) Xu, X.; Goddard, W. A., III *J. Phys. Chem. A* **2004**, *108*, 2305−2313 , and references therein.
(61) Lau, K. H.; Hildenbrand, D. L. *J. Chem. Phys.* **1982**, *76*, 2646−2652.
(62) Zmbov, K. F. *J. Inorg. Nucl. Chem.* **1970**, *32*, 1378−1381.
(63) Andrews, L.; Wang, X. F.; Roos, B. O. *Inorg. Chem.* **2009**, *48*, 6594−6598.
(64) Lyon, J. T.; Hu, H. S.; Andrews, L.; Li, J. *Proc. Natl. Acad. Sci.* **2007**, *104*, 18919−18924.
(65) Arkell, A.; Reinhard, R.; Larson, L. P. *J. Am. Chem. Soc.* **1965**, *87*, 1016−1020.
(66) (a) Flesch, R.; Schurmann, M. C.; Hunnekuhl, M.; Meiss, H.; Plenge, J.; Ruhl, E. *Rev. Sci. Instrum.* **2000**, *71*, 1319−1324 , and references therein. (b) Gong, Y.; Andrews, L. *J. Phys. Chem. A* **2011**, *115*, 3029−3033.